



Local structure of alkalis in mixed-alkali borate glass to elucidate the origin of mixed-alkali effect

Yomei Tokuda, Yuya Takahashi, Hirokazu Masai, Shunichi Kaneko,
Yoshikatsu Ueda, Shigeto Fujimura & Toshinobu Yoko

To cite this article: Yomei Tokuda, Yuya Takahashi, Hirokazu Masai, Shunichi Kaneko, Yoshikatsu Ueda, Shigeto Fujimura & Toshinobu Yoko (2015) Local structure of alkalis in mixed-alkali borate glass to elucidate the origin of mixed-alkali effect, *Journal of Asian Ceramic Societies*, 3:4, 412-416, DOI: [10.1016/j.jascer.2015.09.002](https://doi.org/10.1016/j.jascer.2015.09.002)

To link to this article: <https://doi.org/10.1016/j.jascer.2015.09.002>



© 2015 The Ceramic Society of Japan and
the Korean Ceramic Society



Published online: 20 Apr 2018.



Submit your article to this journal



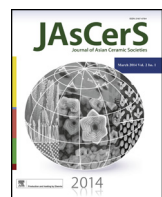
Article views: 49



View Crossmark data



Citing articles: 1 View citing articles



Local structure of alkalis in mixed-alkali borate glass to elucidate the origin of mixed-alkali effect

Yomei Tokuda^{a,*}, Yuya Takahashi^a, Hirokazu Masai^a, Shunichi Kaneko^a, Yoshikatsu Ueda^b, Shigeto Fujimura^c, Toshinobu Yoko^a

^a Institute for Chemical Research, Kyoto University, Gokasho, Uji City, Kyoto 611-0011, Japan

^b Research Institute for Sustainable Humanosphere, Kyoto University, Gokasho, Uji City, Kyoto 611-0011, Japan

^c NARO Tohoku Agricultural Research Center, 50 Harajukuminami, Arai, Fukushima-shi, Fukushima 960-2156, Japan

ARTICLE INFO

Article history:

Received 21 July 2015

Received in revised form 1 September 2015

Accepted 11 September 2015

Available online 14 October 2015

Keywords:

NMR

Borate glass

Mixed-alkali effect

Cs

ABSTRACT

We report the structural analysis of Na^+ and Cs^+ in sodium cesium borate crystals and glasses using ^{23}Na and ^{133}Cs magic-angle spinning nuclear magnetic resonance (MAS NMR) spectroscopy. The composition dependence of NMR spectra of the borate was similar to that of the silicate: (1) the peak position of cesium borate crystals shifted to upfield for structures with larger Cs^+ coordination numbers, (2) the MAS NMR spectra of $x\text{Na}_2\text{O}-y\text{Cs}_2\text{O}-3\text{B}_2\text{O}_3$ ($x=0, 0.25, 0.5, 0.75, 1.0, x+y=1$) glass showed that the average coordination number (CN) of both the alkali cations decreases with increasing $\text{Cs}^+/(Na^++Cs^+)$ ratio. However, the degree of decrement in borates is much smaller than that in silicates. We have considered that the small difference in CN is due to 4-coordinated B, because it is electrically compensated by the alkali metal ions resulting in the restriction of having various coordinations of O to alkali metal.

© 2015 The Ceramic Society of Japan and the Korean Ceramic Society. Production and hosting by Elsevier B.V. All rights reserved.

1. Introduction

Mixed-alkali effect (MAE) is important in glass science because it affects chemical durability, ion conductivity, etc. [1–5]. Several structural models have been presented to explain MAE, for example, the site-mismatch model [3]. Although several kinds of structural analyses were performed to explore this effect, the structural origin of this effect is not fully understood [6,7]. One of the reasons for this is that the structural analyses mainly focused on the glass network and not on the alkalis used in the analyses [8].

Recently, the local structures of alkalis in mixed-alkali silicates have been analyzed using solid-state magic-angle spinning (MAS) nuclear magnetic resonance (NMR) [9,10] and multiple-quantum magic-angle spinning (MQMAS) NMR along with quantum chemical calculations [11]. The analyses revealed that Na^+ ions were heterogeneously distributed in mixed-alkali silicate glasses ($\text{Na}_2\text{O}-\text{K}_2\text{O}-\text{SiO}_2$ glass) and that cations with higher field strengths are likely to occupy the sites with higher basicity, such as

the sites connected with larger number of oxygen atoms or non-bridging oxygen atoms [10,11]. We have considered that one of the reasons for MAE is the heterogeneity of the alkali sites.

Borates are important components for commercial glass and also show MAE [5,12–14], where the coordination number (CN) of B depends on the concentration of the alkali oxide [15]. As is well known, the CN of B gradually changes from three to four with increasing alkali oxide content. The negative charge on B in 4-coordinate site is compensated by the positive charge on the alkali ion. Accordingly, non-bridging oxygen atoms are not generated; however, with further increase in alkali oxide content, bridging oxygen is generated. This behavior is quite different from what is observed in silicate glasses [8]. The main question that arises is what happens to the local structure of the alkali metals in mixed-alkali borate glass; whether there is a heterogeneous distribution of alkali metal ions similar to that observed in silicate glass, and if there is, what is the extent of the heterogeneity. This question is interesting from both technological and scientific points of view.

In this study, we focus on cesium sodium borate glass because ^{23}Na and ^{133}Cs NMR techniques are available to investigate the local structure of the alkalis [10]. We have also performed structural analysis using extended X-ray diffraction (XRD) to support the NMR analysis.

* Corresponding author. Tel.: +81 774384721.

E-mail address: tokuda@noncry.kuicr.kyoto-u.ac.jp (Y. Tokuda).

Peer review under responsibility of The Ceramic Society of Japan and the Korean Ceramic Society.

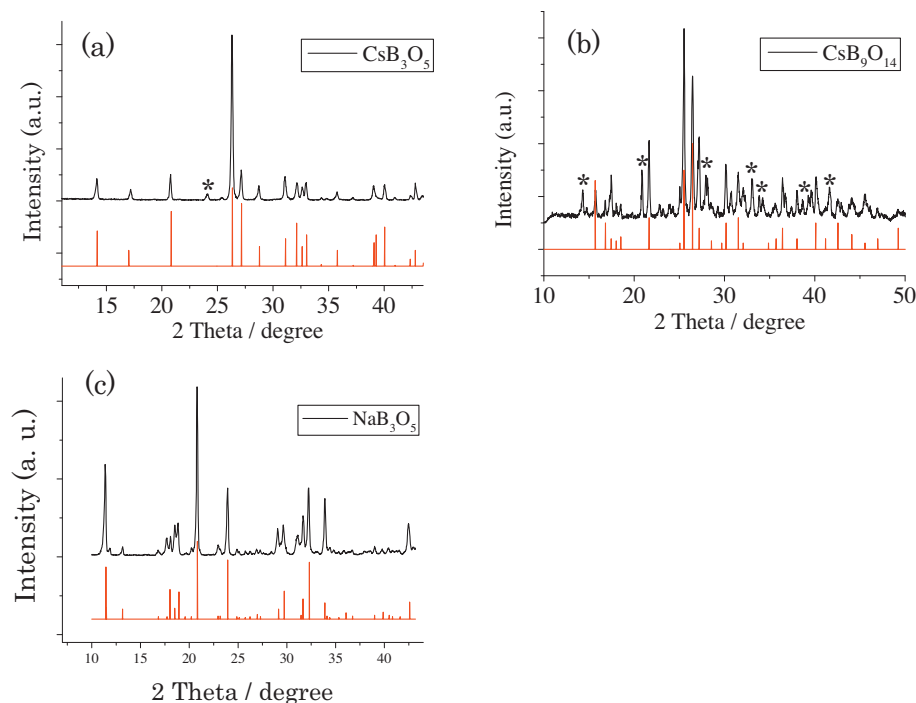


Fig. 1. XRD patterns of cesium borate crystal (a) CsB_3O_5 and (b) $\text{CsB}_9\text{O}_{14}$, and sodium borate crystal (c) NaB_3O_5 . The inset bars are taken from JCPDS cards (27-0107 for CsB_3O_5 , 20-0282 for $\text{CsB}_9\text{O}_{14}$, and 28-1050 for NaB_3O_5). Unknown peaks are indicated by *. CsB_3O_5 crystal is almost single phase, while $\text{CsB}_9\text{O}_{14}$ crystal is contaminated by unknown crystal phase.

2. Experimental

2.1. Preparation of sodium borate and cesium borate crystal

The starting materials, Na_2CO_3 (Wako Pure Chemical Industries, Ltd.), Cs_2CO_3 (Wako Pure Chemical Industries, Ltd.), and $\text{B}(\text{OH})_3$ (Wako Pure Chemical Industries, Ltd.), were used as received.

A NaB_3O_5 crystal was prepared as a reference to define the relationship between the ^{23}Na NMR chemical shifts and the CN of Na^+ [16]. The stoichiometric mixture of the starting materials was melted in a Pt crucible at 1000°C followed by cooling the melt at the rate of $5^\circ\text{C}/\text{min}$ to room temperature to obtain a crystal.

CsB_3O_5 and $\text{CsB}_9\text{O}_{14}$ crystals were also prepared as references to define the relationship between the ^{133}Cs NMR chemical shifts and the CN of Cs^+ [17,18]. The stoichiometric mixtures of the starting materials were melted in a Pt crucible at 1100°C for 20 min. The melts were quenched by water to obtain two kinds of cesium borate glasses; CsB_3O_5 glass was maintained at 580°C for 260 h to obtain the crystal, while $\text{CsB}_9\text{O}_{14}$ glass was maintained at 500°C for 46 h to obtain the crystal.

2.2. Preparation of cesium sodium borate glass

All the glass samples were prepared using the melting method from the above-mentioned starting materials. In a typical process, predetermined quantities of the starting materials were mixed and were melted in a Pt crucible at 1200°C for 30 min. Subsequently, the melts were poured on stainless steel at 200°C . The glasses thus obtained had the composition of $x\text{Na}_2\text{O}-y\text{Cs}_2\text{O}-3\text{B}_2\text{O}_3$ ($x=0, 0.25, 0.5, 0.75, 1.0, x+y=1$). The values of x and y were altered to elucidate MAE. The actual compositions of the glasses were analyzed by X-ray fluorescence spectroscopy (XRF; Rigaku, ZSX 100e). The difference between the batch and analyzed compositions was $<5\%$. Therefore, the compositions of the glasses are referred to as the batch compositions in this report.

2.3. Characterization

The crystal structures of the samples were identified by X-ray diffraction (XRD) analysis (Rigaku, RINT-2100). In addition, the XRD patterns were also simulated from the crystal structure data using VESTA [19].

Solid-state ^{11}B , ^{23}Na , and ^{133}Cs NMR spectra of all the crystals and the glass samples were acquired on a Chemagnetics CMX400 spectrometer using a commercial probe (4 mm). To avoid including water, the samples were crushed into powder and were sealed in sample holders in a glove box. After the measurements, the samples remained in powder form, indicating that they had absorbed no moisture. The rotation speed was set at 10 kHz with an accuracy of ± 10 Hz. When an external field of 9.4 T was applied, the resonance frequencies were approximately 128.4, 103.7, and 53 MHz for ^{11}B , ^{23}Na , and ^{133}Cs , respectively. For each measurement, 90° pulses were set at 3, 2.2, and $10 \mu\text{s}$ for ^{11}B , ^{23}Na , and ^{133}Cs , respectively. The spectra were obtained with cycle times of 5, 1, and 200 s for ^{11}B , ^{23}Na , and ^{133}Cs , respectively. The chemical-shift references were 1-mol/L aqueous solutions of $\text{B}(\text{OH})_3$, NaCl , and CsCl , whose chemical shifts were set at 0 ppm. The spectra of ^{23}Na and ^{133}Cs MAS NMR were normalized, as the total areas are proportional to the alkali metal content observed by NMR. For example, the area of the ^{23}Na MAS NMR spectrum of $0.8\text{Na}_2\text{O}-0.2\text{Cs}_2\text{O}-3\text{B}_2\text{O}_3$ is 4 times larger than that of $0.2\text{Na}_2\text{O}-0.8\text{Cs}_2\text{O}-3\text{B}_2\text{O}_3$. Accordingly, the areas of the spectra can be compared with each other. For the ^{11}B MAS NMR spectra, the peaks were normalized as the heights of the highest peaks were equal.

3. Results and discussion

3.1. XRD analysis of sodium borate and cesium borate crystals

The obtained XRD pattern of crystalline NaB_3O_5 matched with the reported ones [17,18]. The CN of B can be defined as a discontinuous point in the relationship between the B–O distance and the

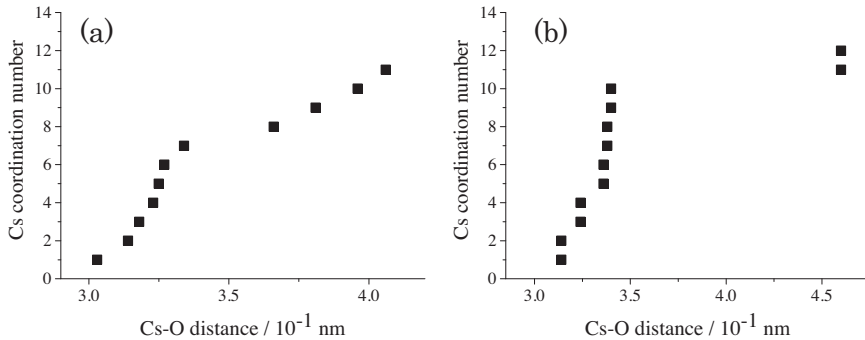


Fig. 2. Relationship between Cs–O distances and coordination numbers in (a) CsB_3O_5 crystal and (b) $\text{CsB}_9\text{O}_{14}$ crystal. The coordination numbers for CsB_3O_5 and $\text{CsB}_9\text{O}_{14}$ crystals are defined as 7 and 10, respectively because there are coordination gaps at 0.35 nm.

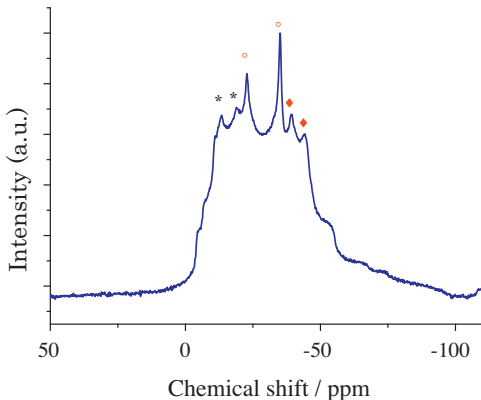


Fig. 3. NMR spectrum of NaB_3O_5 crystal. There are six peaks in the spectrum which is considered to be due to three kinds of Na as *, ◆, and ♦ for CN = 6, 7, and 8, respectively.

number of oxygen atoms near boron [16–18]. According to this definition, CNs of the three kinds of crystallographically independent Na sites that are crystallographically independent in crystalline NaB_3O_5 are 6, 7, and 8.

XRD patterns of crystalline CsB_3O_5 and $\text{CsB}_9\text{O}_{14}$ crystals are shown in Fig. 1(a) and (b). Although there are unknown peaks (*) in the XRD pattern, the main phases are identified as CsB_3O_5 and $\text{CsB}_9\text{O}_{14}$. As a matter of course, it is better to obtain the single phase, i.e., single crystals. However, the XRD patterns of the desired crystals are much larger than those of the unknown ones, indicating that the main peak in the NMR spectra can be assigned to the desired crystal phase. Therefore, these samples are considered pure enough to analyze the relationship between the CN and the chemical shift. The number of oxygen atoms near cesium for CsB_3O_5 and $\text{CsB}_9\text{O}_{14}$ was plotted against the Cs–O distance, as shown in Fig. 2(a) and (b), respectively. The CNs of the cesium atoms are determined to be 7 for CsB_3O_5 and 10 for $\text{CsB}_9\text{O}_{14}$ by the gaps at ~ 0.35 nm.

3.2. NMR spectra of cesium borate crystal and glass

^{23}Na MAS NMR spectrum of the NaB_3O_5 crystal is shown in Fig. 3. As described above, there are three kinds of Na sites in this crystal. However the spectrum had six peaks, probably generated by splitting each peak into two because of quadrupolar coupling. In this study, Na sites of CNs 6, 7, and 8 can be assigned to the first and second peaks, third and fourth ones, and fifth and sixth ones from the right, respectively. Hence, the chemical shift of each Na is defined as the arithmetic average of the split peaks [10]. The calculated chemical shifts were plotted against the CN of Na, as shown in Fig. 4. The linear relationship matches with a previous result obtained for silicate crystals [20]. Linear approximation provided

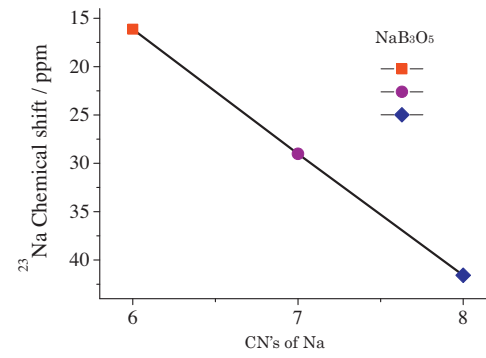


Fig. 4. Relationship between the crystal coordination number (CN) of Na^+ and the chemical shifts of ^{23}Na in the silicate crystals.

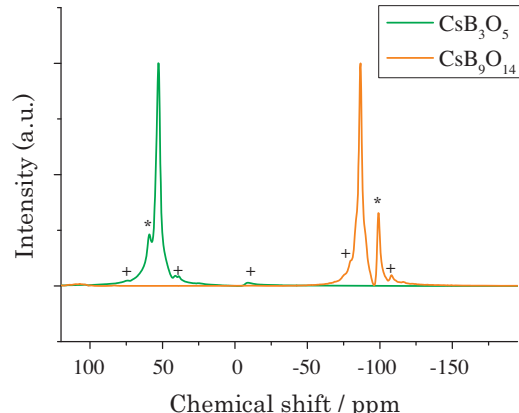


Fig. 5. ^{133}Cs MAS NMR spectra of CsB_3O_5 and $\text{CsB}_9\text{O}_{14}$ crystals. The peaks denoted by * and + are considered to be the unknown crystal phases and the spinning side bands, respectively.

the relationship between the CN of Na and the ^{23}Na chemical shift as follows:

$$\delta_{\text{Na}} = -12.7 \times \text{CN}_{\text{Na}} + 60.1, \quad (1)$$

where δ_{Na} and CN_{Na} are the ^{23}Na chemical shift and the CN of Na, respectively.

^{133}Cs MAS NMR spectra of CsB_3O_5 and $\text{CsB}_9\text{O}_{14}$ crystals are shown in Fig. 5. Both the spectra have two peaks. Small peaks at 60 ppm for CsB_3O_5 and at -100 ppm for $\text{CsB}_9\text{O}_{14}$ are assigned to the contaminated phase that appeared in the XRD patterns (denoted by *). The spinning side bands that also appeared are denoted by

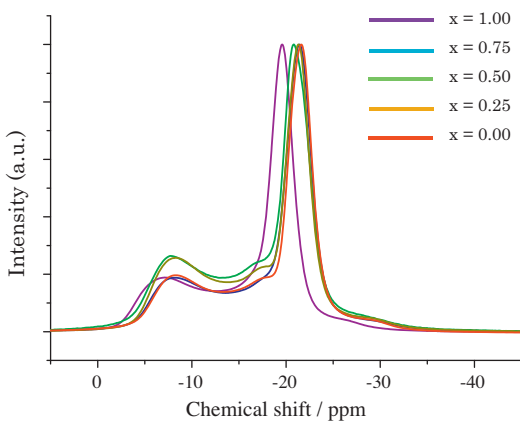


Fig. 6. ^{11}B MAS NMR spectra of $x\text{Na}_2\text{O}-y\text{Cs}_2\text{O}-3\text{B}_2\text{O}_3$ glasses ($x=0.00, 0.25, 0.50, 0.75, 1.00, x+y=1$).

Table 1

Relative amounts of 4-coordinated and 3-coordinated B together with average coordination numbers (CNs). Relative amounts were obtained by the curve fitting.

	4-coordinated B	3-coordinated B	Average CN
$x = 1.00, y = 0.00$	0.65	0.35	3.7
$x = 0.75, y = 0.25$	0.66	0.34	3.7
$x = 0.50, y = 0.50$	0.56	0.44	3.6
$x = 0.25, y = 0.75$	0.57	0.43	3.6
$x = 0.00, y = 1.00$	0.65	0.35	3.6

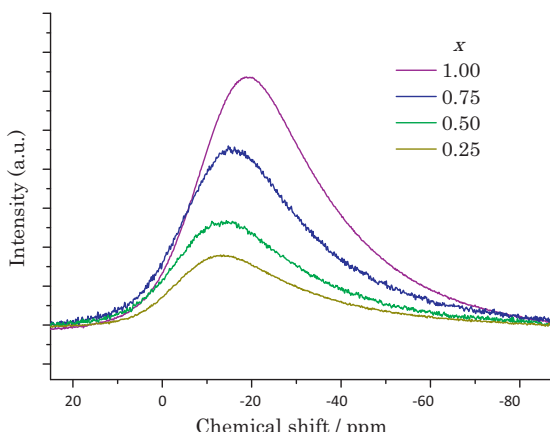


Fig. 7. ^{23}Na MAS NMR spectra of $x\text{Na}_2\text{O}-y\text{Cs}_2\text{O}-3\text{B}_2\text{O}_3$ glasses ($x=0.00, 0.25, 0.50, 0.75, 1.00, x+y=1$).

the symbol +. The relationship between the CN of Cs and the ^{133}Cs chemical shift was also evaluated as follows:

$$\delta_{\text{Cs}} = -47.8 \times \text{CN}_{\text{Cs}} + 388, \quad (2)$$

where δ_{Cs} and CN_{Cs} are the ^{133}Cs chemical shift and the CN of Cs, respectively.

Next, the NMR spectra for the glasses were analyzed. ^{11}B MAS NMR spectra of $x\text{Na}_2\text{O}-y\text{Cs}_2\text{O}-3\text{B}_2\text{O}_3$ glasses are shown in Fig. 6, all of which had a sharp peak at higher magnetic field, assigned to 4-coordinated B, and a broad peak at lower magnetic field, assigned to 3-coordinated B [21]. The area under the peaks assigned to 3- and 4-coordinated B was calculated by spectrum deconvolution with dmfit [22]. The average CNs of B are in the range 3.6–3.7 (Table 1), which are in accordance with a previous report [21]. This result indicated that the variation in alkali content does not affect the network structure composed by borate.

Fig. 7 shows that in the ^{23}Na MAS NMR spectra of $x\text{Na}_2\text{O}-y\text{Cs}_2\text{O}-3\text{B}_2\text{O}_3$ glasses, on replacing Na^+ in the $\text{Na}_2\text{O}-3\text{B}_2\text{O}_3$ glass

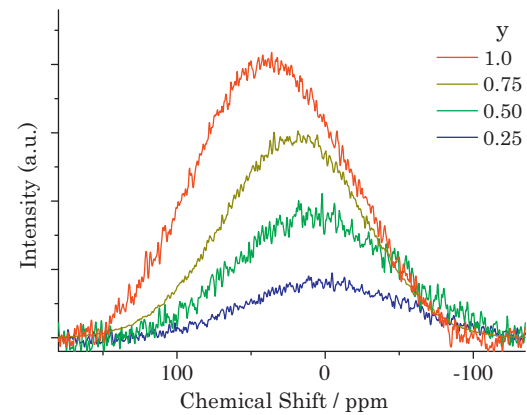


Fig. 8. ^{133}Cs MAS NMR spectra of $x\text{Na}_2\text{O}-y\text{Cs}_2\text{O}-3\text{B}_2\text{O}_3$ glasses ($x=0.00, 0.25, 0.50, 0.75, 1.00, x+y=1$).

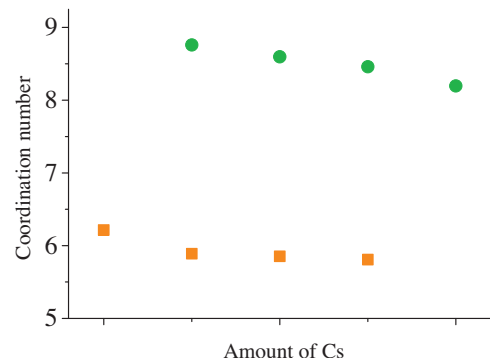


Fig. 9. Average coordination numbers of Na^+ and Cs^+ in $x\text{Na}_2\text{O}-y\text{Cs}_2\text{O}-3\text{B}_2\text{O}_3$ glasses ($x=0.00, 0.25, 0.50, 0.75, 1.00, x+y=1$).

with Cs^+ , the high-magnetic-field component in the NMR spectrum decreases in intensity, similar to the behavior observed for silicate glass [10]. Additionally, as shown in Fig. 8, ^{133}Cs MAS NMR results indicate that the low-magnetic-field component decreases in intensity with decreasing Cs content. Here, we can compare the intensity because the areas of the NMR peaks were proportional to the amount of Cs in the glasses as indicated in Section 2.

Using relationships (1) and (2), the average CNs of Na and Cs were plotted against composition (Fig. 9). In Na-Cs borate glasses, the average CNs of Cs are larger than that of Na, similar to silicate glasses, which is a possible reason for MAE from the viewpoint of the glass structure.

The average coordination of the alkali metals decreased (from 6.5 to 6 for Na^+ and from 9 to 8 for Cs^+) with increasing value of $\text{Cs}^+/(\text{Na}^+ + \text{Cs}^+)$. The decrement was also observed in silicate glass; the CN of Na decreases from 9 to 7 and that of Cs from 14 to 9 [10]. Accordingly, the degree of the decrement in borates is much smaller than that in silicates. This small difference is a major finding of this research. Indeed, in the case of electrical resistance, MAE in borate glass is smaller than that in silicate glass [4,5].

We have considered the small difference in the CN as follows. In the borate glass used in the present study, the majority of the B content is 3-coordinated or 4-coordinated B, which is electrically compensated by the alkali metal ions. This means that the bonding pattern of the alkali metal ions and the borates is face sharing. Accordingly, there are three O atoms at fixed position on one side surrounding the alkali metal ion, resulting in the restriction of having various coordination numbers of O to alkali metal.

4. Conclusion

In conclusion, we have found the similarities and differences in the environment of the alkali metal species in borate and silicate glasses. In this study, we have analyzed the local structure of the alkali ions $^{23}\text{Na}^+$ and $^{133}\text{Cs}^+$ in cesium sodium borate glasses using NMR. To obtain the relationship between CN and chemical shift, we performed NMR analysis on NaB_3O_5 , CsB_3O_5 , and $\text{CsB}_9\text{O}_{14}$ crystals. The relationships were calculated as $\sigma_{\text{Na}} = -12.7 \times \text{CN}_{\text{Na}} + 60.1$ and $\sigma_{\text{Cs}} = -47.8 \times \text{CN}_{\text{Cs}} + 388$. In Na–Cs borate glasses $x\text{Na}_2\text{O}-y\text{Cs}_2\text{O}-3\text{B}_2\text{O}_3$ ($x=0, 0.25, 0.5, 0.75, 1.0$, $x+y=1$), the CNs of both alkali cations (Na^+ and Cs^+) decrease as the value of $\text{Cs}^+/(\text{Na}^+ + \text{Cs}^+)$ increases. This difference in the average CN is considered a structural reason for MAE. In comparison with a previous study, the decrement in the CN of both alkali cations in borate glass is much smaller than that in silicate glass. We considered that this decrement is due to the 4-coordinated B that restricts the variety of coordinated O in the surrounding area of alkalis. In the near future, we plan to perform structural analysis of alkali ions in borosilicate glass in order to understand the mechanism of MAE in commercial glass from the viewpoint of the alkali local structure.

Acknowledgements

This work was supported by the Collaborative Research Program of Institute for Chemical Research, Kyoto University (2015-70, 2014-64) and the Research Institute for Sustainable Humanosphere, Kyoto University.

References

- [1] J.O. Isard, *J. Non-Cryst. Solids*, **1**, 235–261 (1969).
- [2] D.E. Day, *J. Non-Cryst. Solids*, **21**, 343–372 (1976).
- [3] A. Bunde, M.D. Ingram and P. Maass, *J. Non-Cryst. Solids*, **172**, 1222–1236 (1994).
- [4] R. Terai, *J. Non-Cryst. Solids*, **6**, 121–135 (1971).
- [5] Kostyan, *Handbook of Glass Data Part D*, Elsevier (1991).
- [6] S.V. Stolyar, M.Y. Konon, I.A. Drozdova and I.N. Anfimova, *Glass Phys. Chem.+*, **40**, 298–302 (2014).
- [7] J. Habasaki and K.L. Ngai, *Phys. Chem. Chem. Phys.*, **9**, 4673–4689 (2007).
- [8] H. Maekawa, T. Maekawa, K. Kawamura and T. Yokokawa, *J. Phys. Chem.-US*, **95**, 6822–6827 (1991).
- [9] J. Tsuchida, J. Schneider, R.R. Deshpande and H. Eckert, *J. Phys. Chem. C*, **116**, 24449–24461 (2012).
- [10] T. Minami, Y. Tokuda, H. Masai, Y. Ueda, Y. Ono, S. Fujimura and T. Yoko, *J. Asian Ceram. Soc.*, **2**, 333–338 (2014).
- [11] Y. Tokuda, T. Oka, M. Takahashi and T. Yoko, *J. Ceram. Soc. Jpn.*, **119**, 909–915 (2011).
- [12] A. Edukondalu, M. Purnima, C. Srinivas, T. Sripathi, A.M. Awasthi, S. Rahman and K.S. Kumar, *J. Non-Cryst. Solids*, **358**, 2581–2588 (2012).
- [13] M. Kim, C.H. Song, H.W. Choi, Y.S. Yang and Y.H. Rim, *J. Korean Phys. Soc.*, **54**, 950–956 (2009).
- [14] M. Kim, C.H. Song, H.W. Choi, Y.S. Yang and Y.H. Rim, *J. Korean Phys. Soc.*, **55**, 851–857 (2009).
- [15] A.H. Silver and P.J. Bray, *J. Chem. Phys.*, **29**, 984 (1958).
- [16] J. Krogh-Moe, *Acta Crystallogr.*, **B28**, 1571–1576 (1972).
- [17] J. Krogh-Moe, *Acta Crystallogr.*, **13**, 889–892 (1960).
- [18] J. Krogh-Moe, *Acta Crystallogr.*, **23**, 427–430 (1967).
- [19] K. Momma and F. Izumi, *J. Appl. Crystallogr.*, **44**, 1272–1276 (2011).
- [20] X.Y. Xue and J.F. Stebbins, *Phys. Chem. Miner.*, **20**, 297–307 (1993).
- [21] J. Zhong and P.J. Bray, *J. Non-Cryst. Solids*, **111**, 67–76 (1989).
- [22] D. Massiot, F. Fayon, M. Capron, I. King, S. Calvé, B. Alonso, J. Durand, B. Bujoli, Z. Gan and G. Hoatson, *Magn. Reson. Chem.*, **40**, 70–76 (2001).